

Review

Nanocomposite Foams of Polyurethane with Carbon Nanoparticles—Design and Competence towards Shape Memory, Electromagnetic Interference (EMI) Shielding, and Biomedical Fields

Ayesha Kausar ^{1,2,3,*} , Ishaq Ahmad ^{1,2,3}, Tingkai Zhao ^{1,4}, Osamah Aldaghri ⁵ , Khalid H. Ibnaouf ⁵  and M. H. Eisa ⁵

¹ NPU-NCP Joint International Research Center on Advanced Nanomaterials and Defects Engineering, Northwestern Polytechnical University, Xi'an 710072, China

² UNESCO-UNISA Africa Chair in Nanosciences/Nanotechnology, iThemba LABS, Somerset West 7129, South Africa

³ NPU-NCP Joint International Research Center on Advanced Nanomaterials and Defects Engineering, National Centre for Physics, Islamabad 44000, Pakistan

⁴ School of Materials Science & Engineering, Northwestern Polytechnical University, Xi'an 710072, China

⁵ Department of Physics, College of Science, Imam Mohammad Ibn Saud Islamic University (IMSIU), Riyadh 13318, Saudi Arabia

* Correspondence: dr.ayeshakausar@yahoo.com



Citation: Kausar, A.; Ahmad, I.; Zhao, T.; Aldaghri, O.; Ibnaouf, K.H.; Eisa, M.H. Nanocomposite Foams of Polyurethane with Carbon Nanoparticles—Design and Competence towards Shape Memory, Electromagnetic Interference (EMI) Shielding, and Biomedical Fields. *Crystals* **2023**, *13*, 1189. <https://doi.org/10.3390/cryst13081189>

Academic Editors: Yashvir Singh, Nishant Kumar Singh and Erween Abd Rahim

Received: 5 July 2023
Revised: 24 July 2023
Accepted: 25 July 2023
Published: 31 July 2023



Copyright: © 2023 by the authors. Licensee MDPI, Basel, Switzerland. This article is an open access article distributed under the terms and conditions of the Creative Commons Attribution (CC BY) license (<https://creativecommons.org/licenses/by/4.0/>).

Abstract: Polyurethane is a multipurpose polymer with indispensable physical characteristics and technical uses, such as films/coatings, fibers, and foams. The inclusion of nanoparticles in the polyurethane matrix has further enhanced the properties and potential of this important polymer. Research in this field has led to the design and exploration of polyurethane foams and polyurethane nanocomposite foams. This review article reflects vital aspects related to the fabrication, features, and applications of polyurethane nanocomposite foams. High-performance nanocellular polyurethanes have been produced using carbon nanoparticles such as graphene and carbon nanotubes. Enhancing the amounts of nanofillers led to overall improved nanocomposite foam features and performances. Subsequently, polyurethane nanocomposite foams showed exceptional morphology, electrical conductivity, mechanical strength, thermal stability, and other physical properties. Consequently, multifunctional applications of polyurethane nanocomposite foams have been observed in shape memory, electromagnetic interference shielding, and biomedical applications.

Keywords: polyurethane; nanocomposite; foam; shape memory; radiation shielding; biomedical

1. Introduction

Polyurethane is an imperative category of polymers [1]. Polyurethanes possess the superior features of facile processing, chemical constancy, heat stability, and mechanical confrontation. Simple as well as segmented polyurethanes have been developed, having hard and soft segments in the backbone. The physical and covalent crosslinking between the chains has been found to affect the polymer's features and performance [2]. Polyurethanes have been used as important matrices to form foam materials [3]. For this concern, various foaming approaches have been used. Polyurethanes have been employed for high-tech applications ranging from aerospace/automobiles to the electronics and biomedical fields [4–6]. Developments in polyurethane foam materials led to the formation of nanocomposite sponges with nanoparticle reinforcements [7,8]. Here, carbon nanoparticles like graphene and carbon nanotube have been applied as effective nanofillers for foam materials [9–11]. The polyurethane nanocomposite foams are lightweight and have fine elasticity, strength, compression, reversibility, and high-efficiency sponge-related

specific features. The conversion of polyurethane foam to polyurethane nanocomposite foam resulted in the further enhancement of the physical properties of these materials. High-performance polyurethane foams and nanocomposite foams have been produced as low-density efficient nanomaterials for applications related to radiation defense, shape recovery, biomedicine, space, construction, packaging, and other industries [12,13].

This state-of-the-art overview elaborates on the design, properties, and technical performance of polyurethane nanocomposite foams. At first, the fundamentals of polyurethane and polyurethane foams are stated. Afterward, the noteworthy systems and features of polyurethane/nanocarbon nanocomposite foams are illustrated. Polyurethane foams have been prepared as flexible thermoset plastics having open or closed cell structures using chemical or physical blowing agents [14,15]. Additionally, the nanocellular structure or blowing agents can be introduced to form thermoplastic polyurethanes' structures [16,17]. Some essential application areas of these nanocomposite sponges have been elaborated, including stimuli-responsive, electromagnetic interference (EMI) radiation shielding, and biomedical materials and systems. For polyurethane foams, some literature review reports have been observed, such as a review article by Sang et al. [18] on interface-engineered magnetic EMI-shielding polyurethane foams. However, to the best of our knowledge, this unique and comprehensive review has an entirely novel outline, design, selected literature, and conforming aspects of polyurethane nanocomposite foams, especially covering three important technical areas (shape memory, EMI shielding, biomedical field) in one place. Consequently, this all-inclusive article will definitely be helpful for field researchers seeking important future aspects and different application areas of these important materials.

2. Polyurethane and Polyurethane Foam

Polyurethanes form a significant class of polymers [19]. Polyurethanes possess urethane functionalities usually formed via the reaction of isocyanate ($R-(N=C=O)_n$) and hydroxyl ($R-(OH)_n$) groups. Polyurethane has been produced in film, powder, or elastomeric forms. Polyurethanes have been frequently prepared using the solution technique, in situ procedure, and other facile methods [20]. Segmented polyurethane is an essential form of polyurethanes [21,22]. These polymers contain soft and hard segments in the backbone. Soft segments have flexible polyols in structure, whereas hard segments have isocyanate linkages in the units. Hard and soft segments in polyurethanes may develop physical interactions (π - π stacking, hydrogen bonding, van der Waals interactions) and covalent linking between chains [23]. An interesting property of polyurethanes is that these polymers exist both as thermoplastic and thermoset forms. Hence, carefully designed polyurethanes have superior thermal constancy, flame resistance, mechanical stability, chemical stability, and other desired characteristics [24]. High-performance polymers have several technological applications such as electronics [25], engineering and structural materials [26], biomaterials [27], etc. In nanocomposite form, polyurethane matrices have been filled with various inorganic and organic nanoparticles. Polyurethanes have a very fine capability to develop foam or sponge materials. Polyurethane foam can be obtained via the foaming of polyurethane matrix [28]. Polyurethane foams have been developed for varying domestic, transportation, and industrial areas [29]. Polyurethane foams may have open cell or close cell morphology [30,31]. Saint-Michel et al. [32] reported obtaining polyurethane foam by employing 4,4'-diphenylmethanediisocyanate and polypropylenes triol monomers. A supercritical carbon dioxide foaming technique was used to form the polyurethane foam [33]. Scanning electron microscopy-based microstructural analysis revealed consistent closed shell structure [34]. High-performance sponges have lightweight, thermal conduction, and non-flammability characteristics [35–37]. Heat stability and barrier characteristics of polyurethane foams have been investigated [38,39]. Remarkable properties of polyurethane sponges led to applications in aerospace, automotive, packaging materials, biomedical, etc. [40–42]. Lately, numerous nanoparticles have been filled in polyurethane matrices to design nanocomposite foams [43,44].

3. Polyurethane-Derived Nanocomposite Foam

3.1. Polyurethane- and Graphene-Based Nanocomposite Foam

Graphene is a one-atom-thick nanocarbon nanosheet with sp^2 hybridized atoms of two-dimensional nanostructures [45]. Due to its unique structure, it has a high specific surface area and superior physical features such as electron transportation, mechanical stability, heat conduction, and chemical stability [46]. Graphene oxide is an imperative derivative of graphene [47,48]. It contains oxygen-rich functionalities on its surface, such as hydroxyl, carboxylic acid, carbonyl, ketonic groups, and others [49,50]. Similar to other polymers, polyurethanes have been used as matrices for graphene nanofillers [51]. Moreover, the polyurethane foam matrix has been reinforced with graphene [52,53]. Adding graphene or graphene oxide resulted in the improvement of mechanical, thermal, conductivity, and other physical characteristics of polyurethane nanocomposite foams [54]. Consequently, various polyurethane/graphene nanocomposite foams have been fabricated and investigated [55,56]. Jiang et al. [57] developed thermoplastic polyurethane nanocomposites with graphene oxide and reduced graphene oxide nanofillers. Figure 1 shows the nanocomposite formation and then the foaming of thermoplastic polyurethane/reduced graphene oxide materials. The solution impregnation method was used for coating the reduced graphene oxide with thermoplastic polyurethane particles. Graphene oxide was formed via the modified Hummers method [58], and L-ascorbic acid was applied to convert graphene oxide to reduced graphene oxide [59]. Consequently, graphene oxide nanoparticles were coated on thermoplastic polyurethane and reduced in situ using L-ascorbic acid. Initially, the nanocomposite powder was developed using vacuum filtration and freeze-drying methods. Hydrogen bonding interactions between carboxyl and urethane functionalities of polyurethane and oxygenated functionalities of graphene oxide were responsible for overall nanocomposite formation. The in situ reduction mechanism is given in Figure 2.

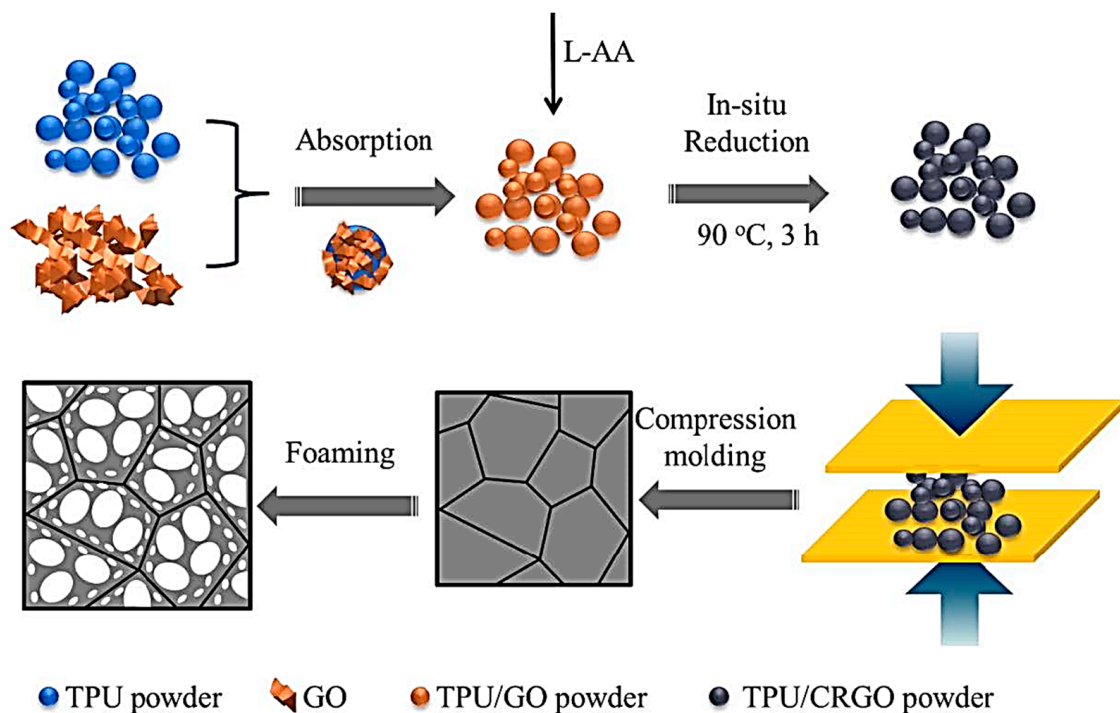


Figure 1. Schematic showing the fabrication process of TPU/RGO nanocomposite foams [57]. L-AA = L-ascorbic acid; TPU = thermoplastic polyurethane; GO = graphene oxide; TPU/GO = thermoplastic polyurethane/graphene oxide; TPU/RGO = thermoplastic polyurethane/reduced graphene oxide; TPU/CRGO = thermoplastic polyurethane/reduced graphene oxide through compression molding. Reproduced with permission from Elsevier.

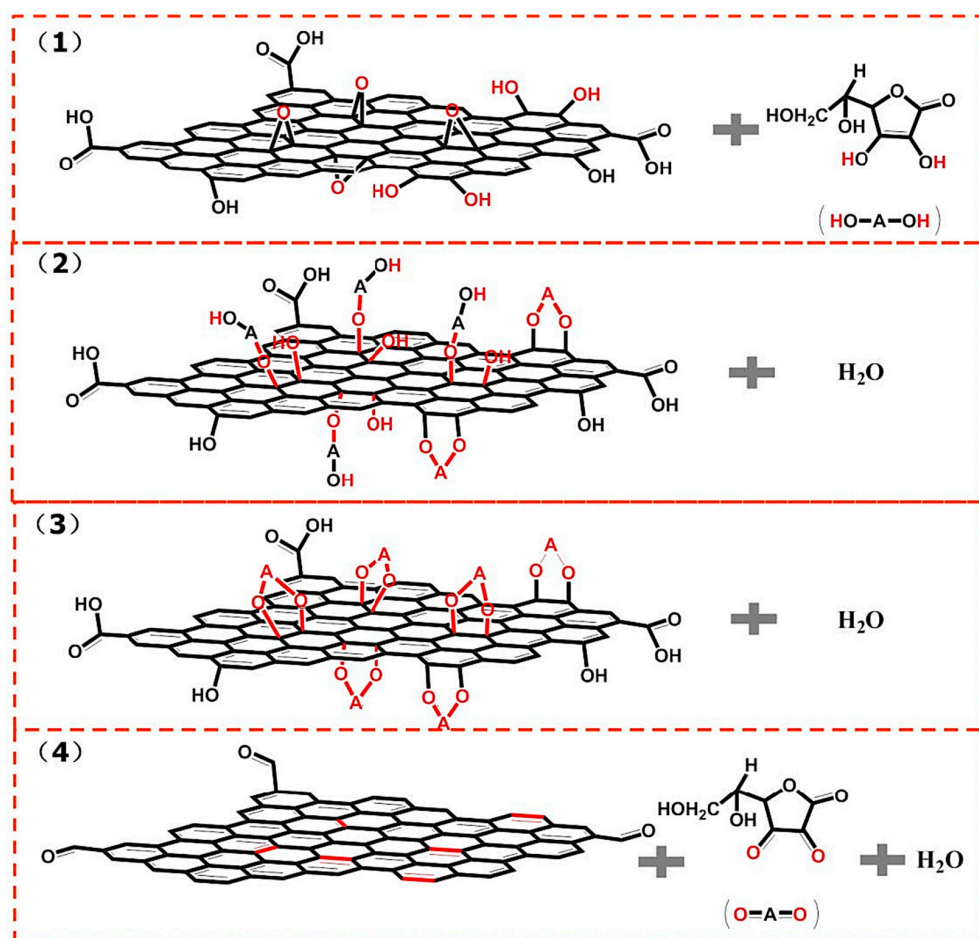


Figure 2. Schematic drawing of in situ reduction of graphene oxide using L-ascorbic acid: (1,2) reaction of L-ascorbic acid and graphene oxide; (3) water addition to modified graphene oxide; (4) reaction of reduced graphene and L-ascorbic acid [57]. Reproduced with permission from Elsevier.

The L-ascorbic acid was considered an ecofriendly reducing agent, compared with the hydrazine-type hazardous reducing agent for graphene oxide. Afterward, the supercritical CO₂ foaming method was used for the formation of the polyurethane/reduced graphene oxide nanocomposite foam [60]. The nanocomposite was placed in a high-pressure vessel and flushed with low-pressure CO₂. Consequently, the sample was exposed to supercritical CO₂ under 14 MPa at 80 °C. After saturation of the sample with supercritical CO₂, the reaction vessel was depressurized and cooled, and foamed samples were obtained. The electrical conductivity of nanocomposite foam was found to be $2.53 \times 10^{-1} \text{ Sm}^{-1}$. Consequently, including 3.17 vol.% reduced graphene oxide nanofiller resulted in an electromagnetic shielding effectiveness of about 22 dB.

Li et al. [61] reported on polyurethane/graphene nanocomposite foam as an EMI shielding material. Figure 3 shows the procedure for the development of polyurethane/graphene nanocomposite foam. In this process, polyurethane/graphene nanocomposite was obtained via a solution route and precipitated to obtain the product. Then, nanocomposite foam was developed by re-dissolving the precipitate in dimethylformamide and using a solvent-induced phase separation route. As obtained polyurethane/graphene nanocomposite foam had high shielding effectiveness of ~23–24 dB.

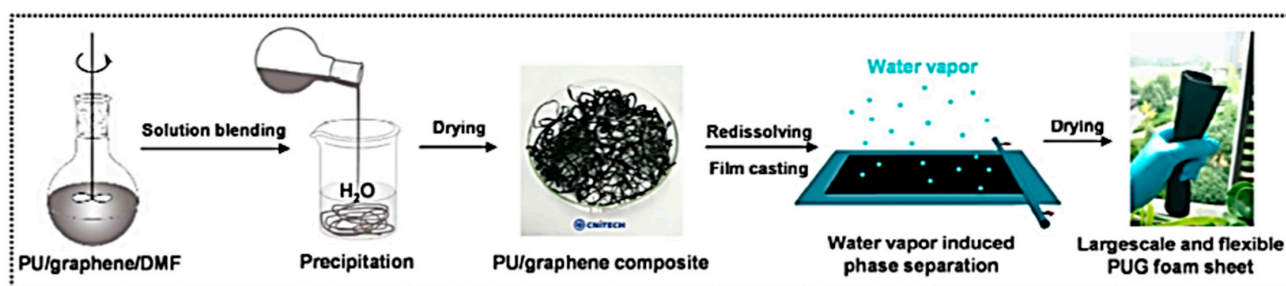


Figure 3. Schematic design for the fabrication of polyurethane/graphene (PU/G) nanocomposite foam [61]. DMF = dimethyl formamide; PU = polyurethane. Reproduced with permission from Elsevier.

Feng and co-workers [62] used ultrasonication, freeze drying, and solvent extraction techniques to develop polyurethane/graphene nanocomposite foams. The porous microstructure and compressive stress properties of nanocomposite foams were examined. Investigations into the electric conductivity and strength features of polyurethane/graphene nanocomposite foams were explored by Chen et al. [63]. Similarly, Hodlur and co-workers [64] investigated electron conduction, compressibility, and flexibility properties of polyurethane/graphene oxide nanofoam materials [65]. These spongy nanomaterials also have fine sound absorption characteristics, according to Kim et al. [66]. These physical properties of three-dimensional nanostructures were found to enhance with nanofiller addition. Polyurethane nanocomposite foams with graphene and graphene oxide nanofillers have a three-dimensional consistent flexible network microstructure for advanced technical features.

3.2. Polyurethane- and Carbon Nanotube-Derived Nanocomposite Foam

Carbon nanotube is also an important one-dimensional nanocarbon nanostructure consisting of sp^2 hybridized atoms [67,68]. It can be imagined as a rolled-up nanosheet of graphene [69,70]. However, several overlapping graphene cylinders form multi-walled carbon nanotubes. Similar to graphene, carbon nanotubes have been reinforced in polymers to achieve enhancement in the nanocomposite properties [71,72]. In polymeric foams, carbon nanotubes can be included as efficient nanofillers to enhance the valuable properties of three-dimensional nanostructures [73,74]. Similarly, the polyurethane foam matrix has been reinforced with a carbon nanotube to attain the desired foam materials [75]. A one-dimensional nanotube is a fine nanofiller to form a three-dimensional network in polymeric sponges. The resulting foam has enhanced structural, strength, compressibility, electrical, and other physical properties [76]. Consequently, polyurethane- and carbon nanotube-derived foams have been applied for technical applications. Yan and coworkers [77] fabricated polyurethane- and carbon nanotube-based nanocomposite foams. Three-dimensional nanostructures have been explored for electrical conductivity and mechanical performance. Nanocomposite foams revealed percolation thresholds of 1.2 wt.% due to an interlinked conducting network in the sponge matrix [78,79]. A polyurethane/carbon nanotube nanocomposite foam system depicted an electrical conductivity of $0.23 \text{ S}\cdot\text{cm}^{-1}$, as reported by You et al. [80]. For this system, a decrease in electron transportation was observed by enhancements in nanofiller contents and aggregation [81,82]. Madaleno et al. [83] reinforced polyurethane foam with a carbon nanotube- and montmorillonite-based hybrid nanofiller. The hybrid nanofiller was reinforced in polyurethane foam via an in situ process. Even small amounts of nanofillers have been found to enhance the thermal and compression features of nanocomposites. Huang et al. [76] designed thermoplastic polyurethane and carbon nanotubes resulting in nanocomposite foams. Directional freeze drying was used to form low-density and flexible foams with fine compression and reversibility properties. Figure 4 shows a directional freeze-drying process for developing aligned nanocomposite foams. For this purpose, ultrasonication and 1,4-dioxane solvents have been applied for carbon nanotube dispersion. A thermally insulated container and cylindrical metal block were used in the foaming setup. An aligned porous structure was obtained after freeze

drying. Figure 5 depicts the formation of aligned unfilled thermoplastic polyurethane foam and thermoplastic polyurethane/carbon nanotube nanocomposite foam. Scanning electron microscopy images of aligned unfilled and filled thermoplastic polyurethane foams were scanned. Uniquely aligned samples revealed fine morphology due to the formation of regularly interlinked nanocomposite nanostructure. The freeze-drying method has been found to be effective in developing a unidirectional ladder-like solidification in foam structures. Figure 6 shows a simple comparison of the compression and reversibility processes for thermoplastic polyurethane/carbon nanotube nanocomposite foams. For aligned foam structures, the reversibility process was found to be much smoother than the disordered foam nanocomposite structure.

Zhai et al. [84] also prepared polyurethane/carbon nanotube nanocomposite foams. Nanocomposite foams were developed using the water blown technique [85–87]. Figure 7 illustrates the compression stress–strain features of polyurethane/carbon nanotube nanocomposite foams with different carbon nanotube contents. Adding carbon nanotube considerably improved the compressive stress properties of nanocomposite foams, along with enhancements in flexibility properties [88]. Espadas-Escalante and co-workers [89] studied the thermal conductivity as well as the non-flammability features of polyurethane/carbon nanotube nanocomposite foams. Including nanotube nanofiller increased the thermal conductivity as well as the non-flammability properties of the foams. Moreover, these nanocomposite foams were investigated for electrical conductivity and compressibility characteristics [90]. Further research may reveal several other potential features of polyurethane/carbon nanotube nanocomposite foams.

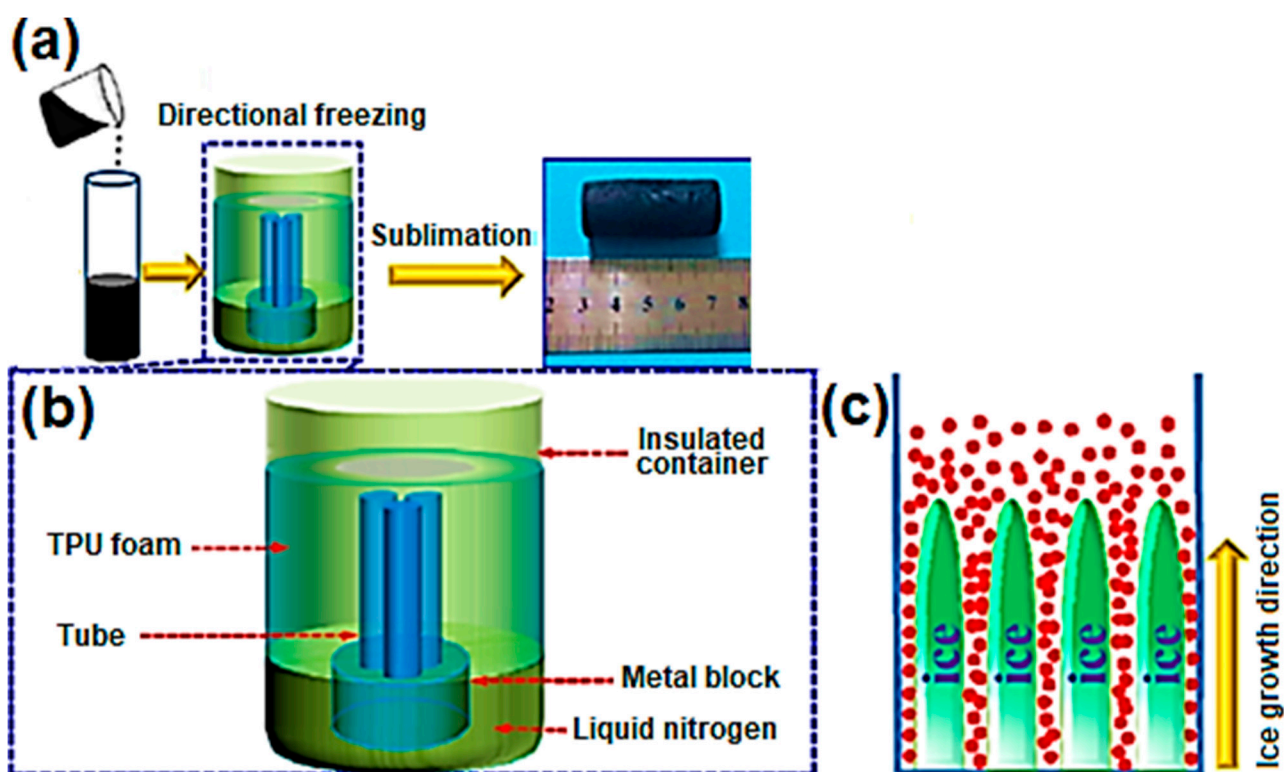


Figure 4. (a) Fabrication process of aligned thermoplastic polyurethane/carbon nanotube nanocomposite foam; (b) graphic illustration of the directional-freezing device; and (c) the directional freezing process [76]. Reproduced with permission from ACS.

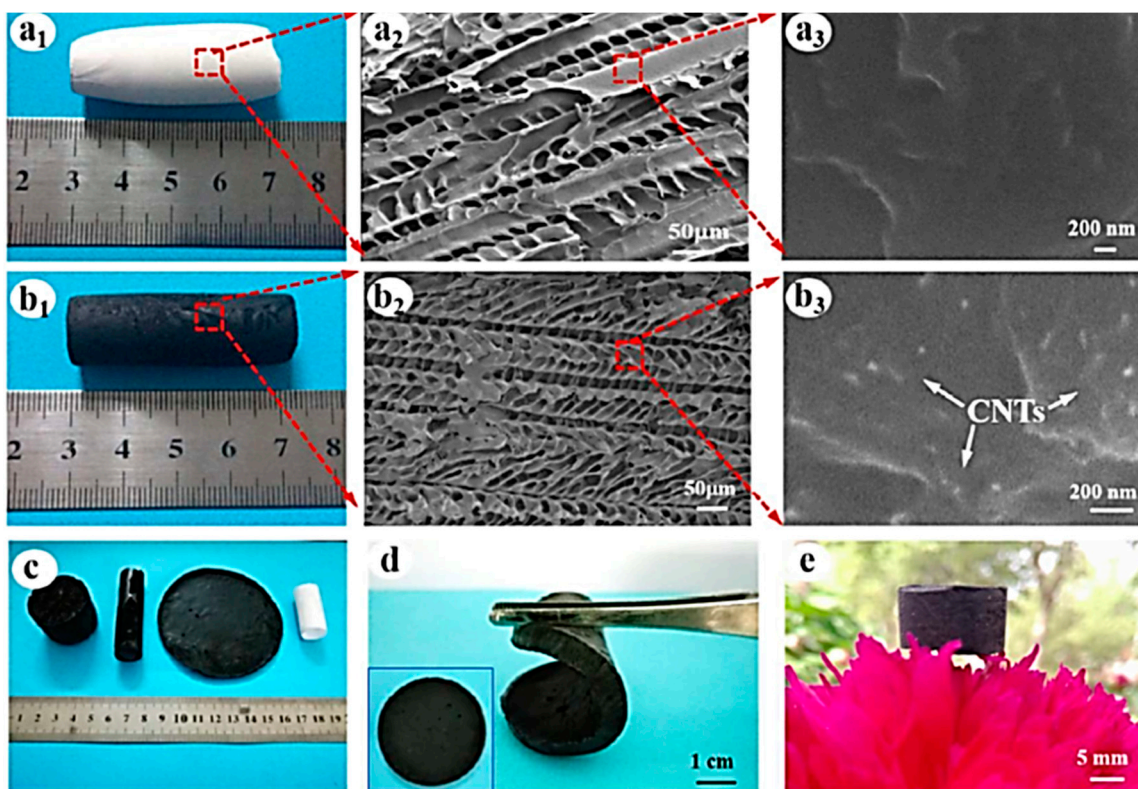


Figure 5. Scanning electron microscopy images of (a1–a3) the unfilled thermoplastic polyurethane foams, (b1–b3) thermoplastic polyurethane/carbon nanotube nanocomposite foams, and (c–e) various shapes of aligned conducting thermoplastic polyurethane/carbon nanotube nanocomposite foams prepared [76]. CNTs = carbon nanotubes. Reproduced with permission from ACS.

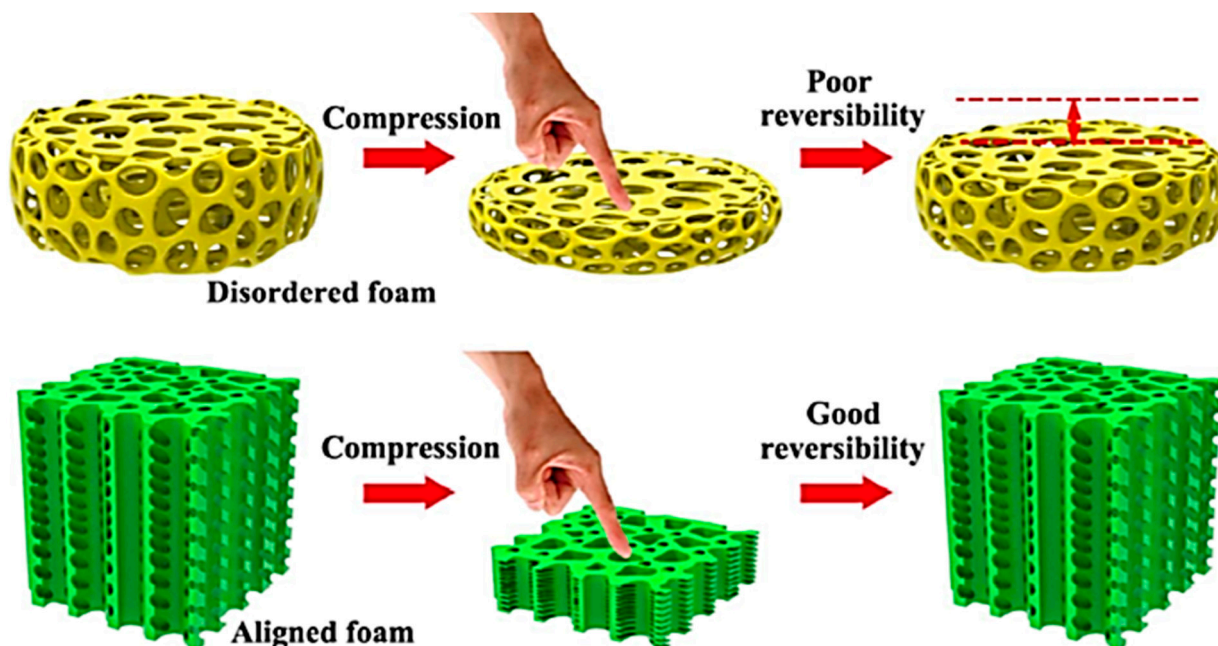


Figure 6. Schematic diagram of the comparison of reversibility process of the aligned and disordered conductive thermoplastic polyurethane/carbon nanotube nanocomposite foams [76]. Reproduced with permission from ACS.

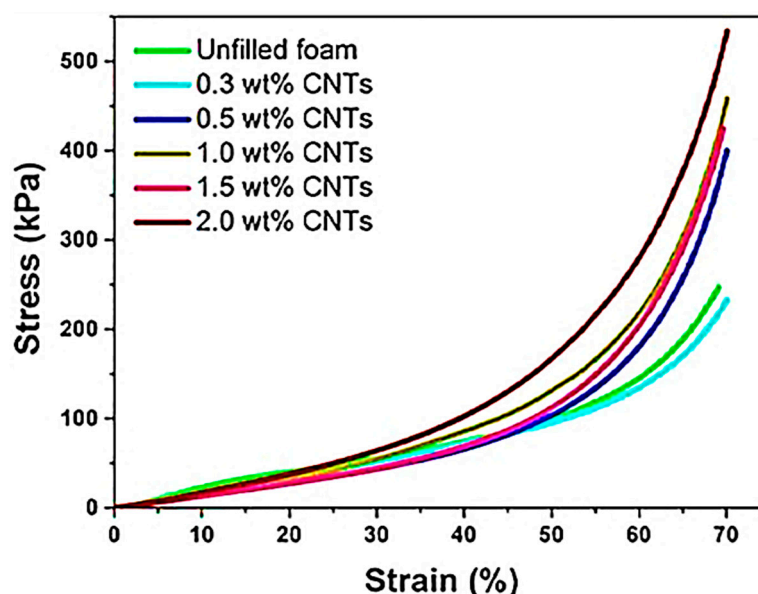


Figure 7. Compression stress–strain properties of the polyurethane/carbon nanotube nanocomposite foams having varying carbon nanotube contents [84]. Reproduced with permission from Elsevier.

4. Technical Significance of Polyurethane Nanocomposite Foam

4.1. Shape Memory Nanomaterials

Shape memory or stimuli-responsive polymers have been recognized as significant smart materials [91–93]. A shape memory polymer has the capability to deform and then recover its original shape under the effects of heat, light, electric field, pH, force effect, moisture, etc. [94–96]. Furthermore, these shape recovery polymers have high-efficiency characteristics such as electron conduction, strength, heat constancy, glass transition/melting temperature, non-flammability, and other properties [97,98]. High-performance polymer foams reveal essential stimuli-responsive features under environmental effects. Congruently, polyurethane foams have revealed stimuli-responsive applications [99,100]. Singhal et al. [101] developed polyurethane foam with 1,6-diisocyanatohexane, N,N,N',N'-tetrakis(2-hydroxypropyl)ethyl-enediamine, and 2,2',2''-nitrilotriethanol reactants. Ensuing polyurethane foams had a glass transition temperature of about 45–70 °C. Polyurethane foams depicted fine thermo-responsive shape memory influence [102,103]. In these materials, 97–98% shape recovery has been attained. Kim and co-workers [104] fabricated shape memory polyurethane- and carbon nanotube-derived nanocomposite foams via a microwave heating technique. The inclusion of carbon nanotubes also resulted in superior thermal and mechanical characteristics. Microwave exposure was used to study thermo-responsive behavior. Kang and colleagues [105] researched polyurethane nanocomposite foam prepared with 2,4/2,6-toluene diisocyanate and polypropylene glycol reactants. As obtained polyurethane foams were reinforced with carbon nanotube nanofiller [106]. A nanocomposite foam was designed using the one-shot foaming technique and by adding a blowing agent [107]. In addition, shape memory polyurethane/graphene nanocomposite foams have also been explored for the shape memory effects [108]. Zhou et al. [109] developed shape memory polyurethane with graphene and carbon nanotube nanofillers. Figure 8 discloses the compression recovery steps of polyurethane/graphene foams via stress–strain analysis at different set strains of 20 to 90%. Moreover, the cyclic stress–strain performances of nanocomposite foams were analyzed at 50% strains. These tests revealed good elasticity and flexibility properties.

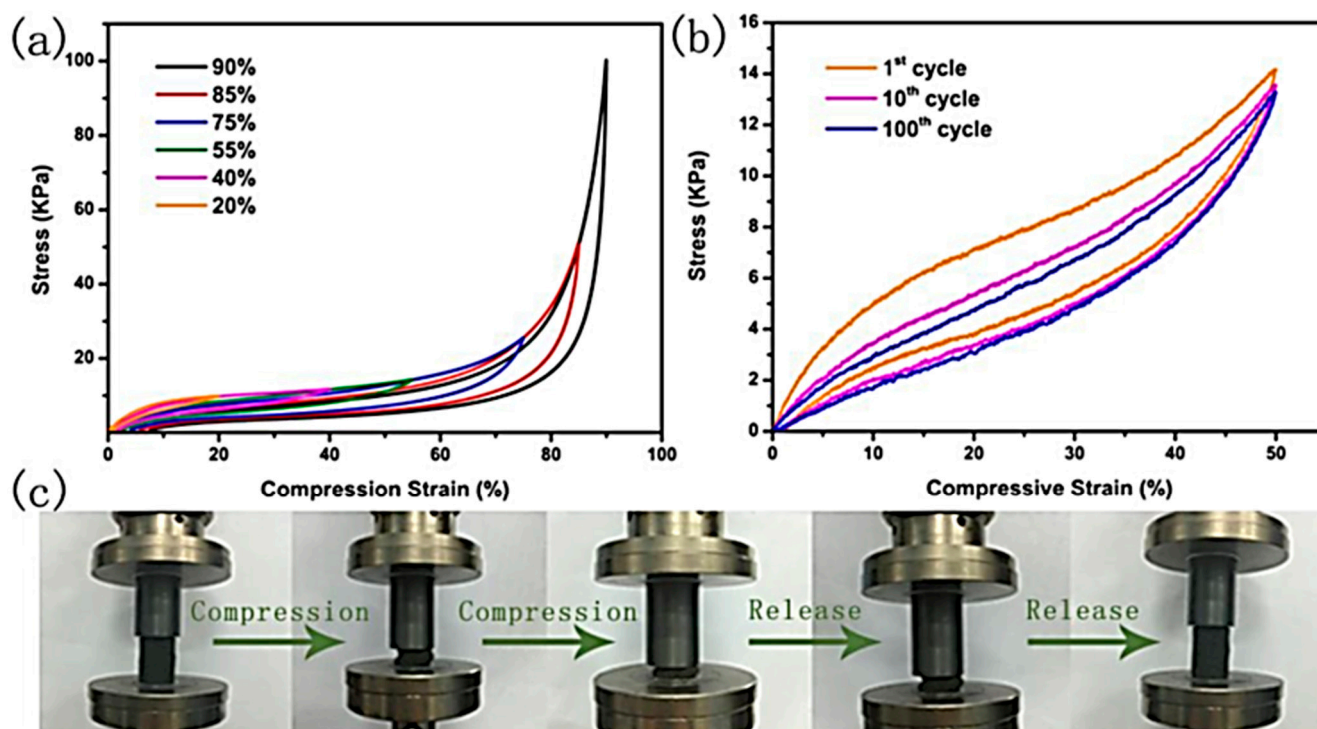


Figure 8. The compression recovery process of polyurethane/graphene foam: (a) stress–strain curves of foams with different set strains of 20 to 90%; (b) cyclic stress–strain curves of foams at 50% strain; (c) compressing and releasing process showing recovery of original shape after compression by more than 90% [109]. Reproduced with permission from Elsevier.

Figure 9 depicts the stimuli response of three-dimensional polyurethane nanocomposite foams filled with graphene (8 wt.%) and carbon nanotube (3 wt.%). As obtained samples were heated using a power source at 100 V. An efficient shape recovery effect was observed due to the heating effect. To form a temporary U shape, the sample was heated to 60 °C, bent, and the shape was preserved by cooling at 0 °C. The original shape was recovered in 150 s under 100 V. Shape memory nanocomposite foams showed technical applications in the space sector, sensors, actuators, electronics, biomedical devices, and related smart applications [110–112].

4.2. Electromagnetic Interference Shielding

A significant utility of polyurethane-based nanocomposite foams has been studied for electromagnetic interference (EMI) shielding [113,114]. Nanocomposite foams have low density, facile foaming methods, and fine electron conduction responsible for high EMI shielding effects [115]. Additionally, the EMI protection phenomenon depends on the nanofiller type, amount, scattering, etc. In particular, carbon nanoparticle additives such as graphene and carbon nanotube in polyurethane foams have been found effective. Such EMI shields possess high electrical conductivity, dielectric features, and EMI shielding characteristics. Li and researchers [116] researched waterborne polyurethane and carbon nanotube-derived nanocomposite foams for radiation shielding purposes. Nanocomposite foams have pointedly high electrical conductivities of 362 Sm^{-1} due to the formation of an interconnecting nanotube network in the foam structures. Consequently, nanocomposite foams had fine shielding effectiveness of about 25 dB. Gavvani et al. [117] developed polyurethane and reduced graphene oxide-based nanocomposite foams for EMI shielding. Nanocomposite foams prepared were elastic and low density. Moreover, good graphene dispersion and homogeneous morphology were obtained due to the processing technique used. Nanofiller dispersion, regular microstructure, and material thickness enhanced the absorption-based EMI shielding of foams. Graphene developed a fine interrelating

network in the three-dimensional foam architecture to promote an electron percolation system. The polyurethane/reduced graphene oxide nanocomposite foam revealed a considerably high electrical conductivity of 4 Sm^{-1} and a superior EMI shielding effectiveness of $\sim 253 \text{ dB}$. Jiang et al. [57] produced low-density and elastic thermoplastic polyurethane and reduced graphene oxide-derived nanocomposite foams using the supercritical CO_2 foaming technique and simple non-foamed nanocomposites for EMI shielding. Figure 10 shows the EMI shielding mechanism of polyurethane/reduced graphene oxide nanocomposite and polyurethane/reduced graphene oxide nanocomposite foams in the X-band region. In nanocomposite foams, the formation of an interconnected nano-cellular structure has facilitated incident microwave absorption via multiple reflections and scattering phenomena. Polyurethane/reduced graphene oxide nanocomposite foams with 3.17 vol.% reduced graphene oxide had high electrical conductivity due to interlinked network formation. Consequently, a high EMI shielding effectiveness of 21.8 dB was attained. In particular, the absorption mechanism of nanocomposite foam was dependent upon the EMI shielding effect.

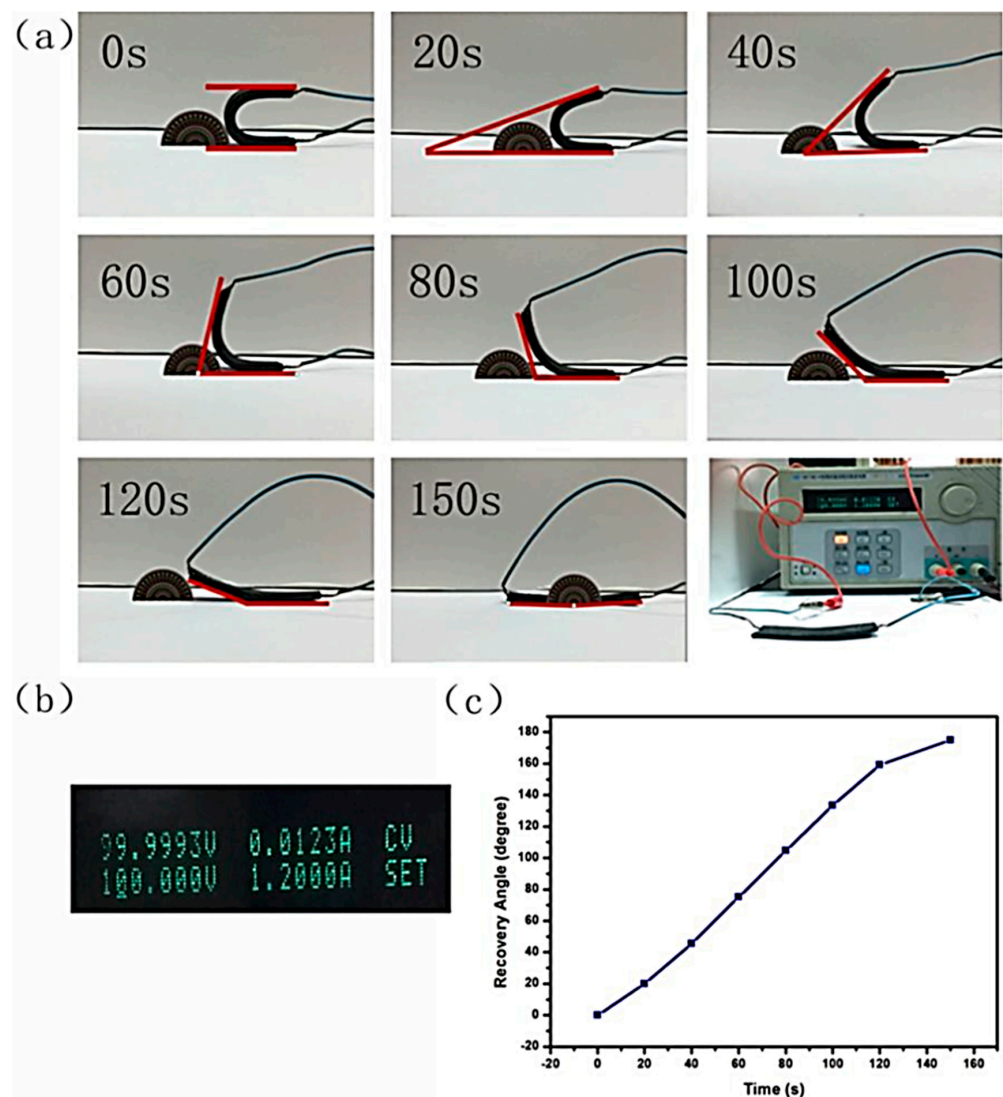


Figure 9. (a) Shape recovery process of three-dimensional polyurethane nanocomposite foam with graphene (8 wt.%) and carbon nanotube (3 wt.%) under 100 V; (b) magnification of the screen reading; and (c) the relationship of recovery time vs. recovery angle [109]. Reproduced with permission from Elsevier.

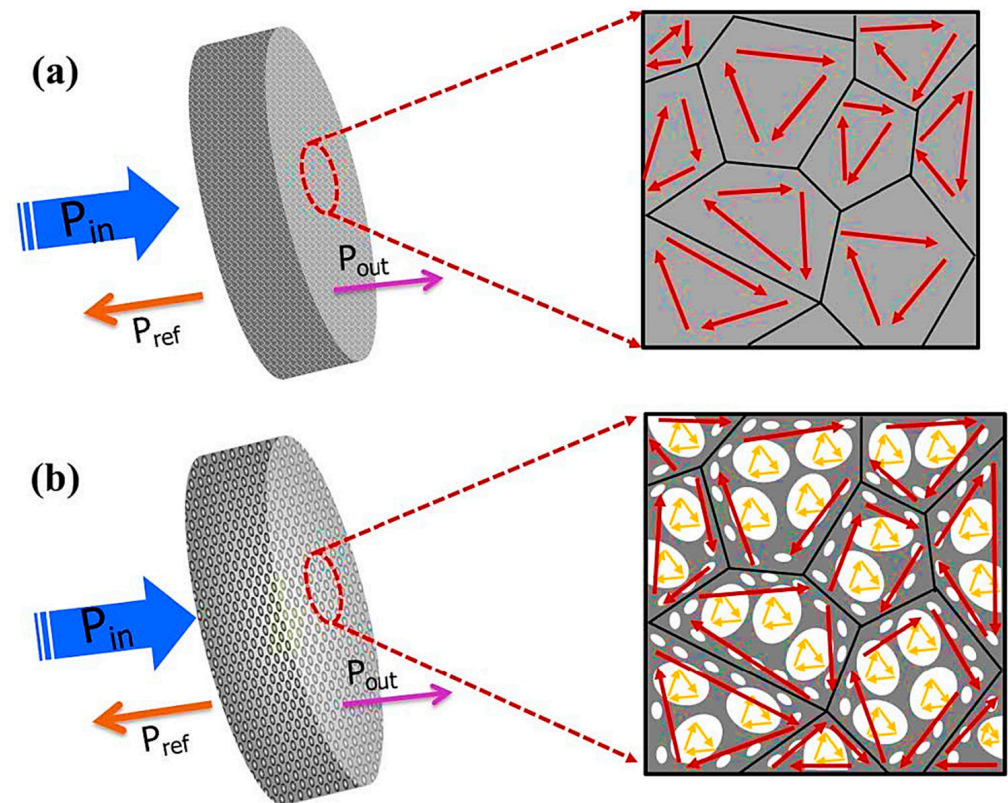


Figure 10. Representation of electromagnetic waves transfer across (a) the thermoplastic polyurethane/reduced graphene oxide nanocomposite and (b) the thermoplastic polyurethane/reduced graphene oxide nanocomposite foam [57]. Red arrows = Reflected radiations; yellow arrows = multiple internal reflections. Reproduced with permission from Elsevier.

Li et al. [61] fabricated multi-layered thermoplastic polyurethane/graphene sandwiched nanocomposite foams by piling up several single-layered thermoplastic polyurethane/graphene nanocomposite foams. Sandwiched thermoplastic polyurethane/graphene nanocomposite foam structures had improved absorption features for incident radiation. With an increasing thickness of the EMI shielding foam, reflection loss was observed due to the constructive interference effects. The EMI shielding of thermoplastic polyurethane/graphene sandwiched nanocomposite foams was observed in the region of the Ku-band (Figure 11). The shielding effectiveness of foam materials was found to increase with graphene loading. At 20 wt.% graphene nanofiller addition, EMI shielding effectiveness was found in the range of 17 to 21 dB. Improved effectiveness was experiential due to the formation of fine conducting links of graphene additives. On the other hand, unfilled polyurethane was insulating in nature and translucent toward electromagnetic radiations. The EMI shielding mechanism was found to depend on shielding effectiveness absorptions (SE_A) as well as shielding effectiveness reflections (SE_R). Both SE_A and SE_R were dependent upon graphene addition and found to enhance with increasing graphene contents.

Table 1 shows the electrical conductivity and EMI shielding effectiveness of polyurethane nanocomposite foam. A correlation between electrical conductivity and radiation shielding properties has been observed. High EMI SE was attributed to strong interfacial interactions between matrix–nanofiller leading to the high electrical conductivity of the system. Carbon nanofiller efficiently developed conducting interfaces causing an interfacial polarization effect. Due to possible relaxation modes and interfacial polarization effects, resulting dielectric losses caused high microwave absorption and increased EMI SE phenomenon.

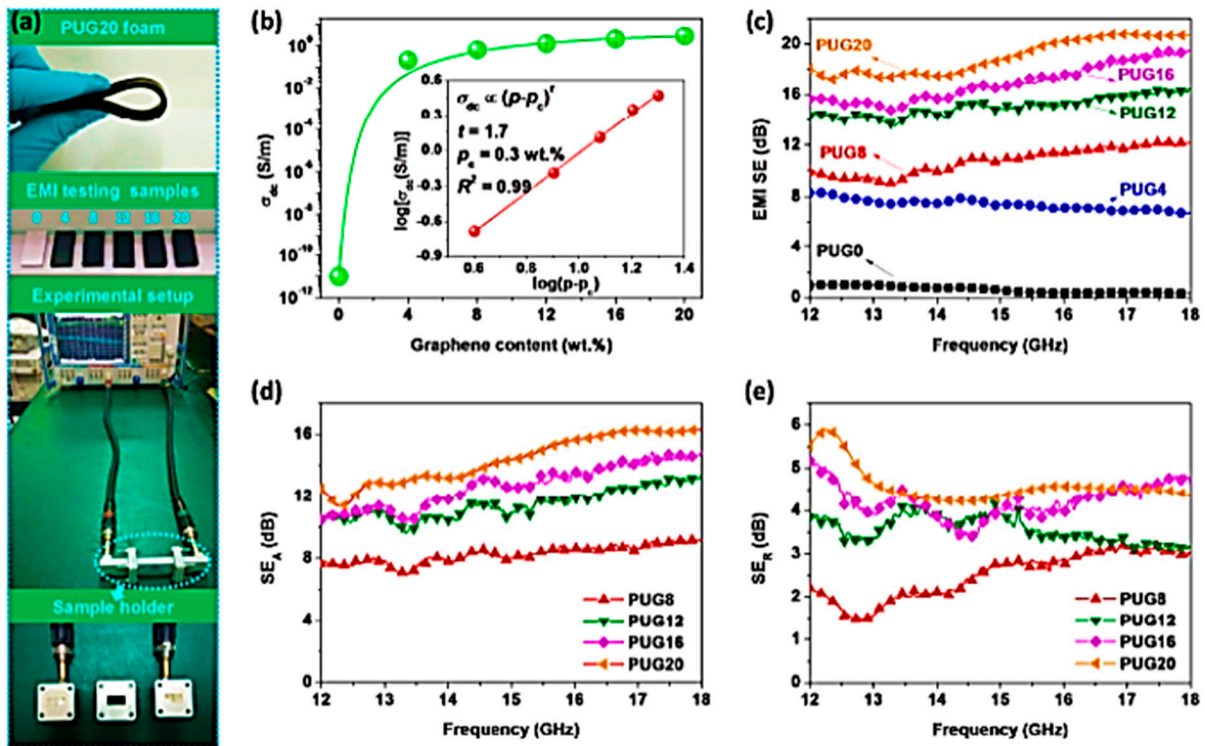


Figure 11. (a) Digital images of polyurethane/graphene foam, electromagnetic samples with varying graphene contents, experimental setup, and the sample holder used; (b) DC conductivity (σ_{dc}) of polyurethane/graphene foam foams, where the inset shows the log-log plot of σ_{dc} versus $(p-p_c)$, and the solid line shows a fit to the measured data using relationship of $\sigma_{dc} \propto (p-p_c)^t$; and (c–e) shielding effectiveness (SE) total, SE absorption (SEA), and SE reflection (SER) of the polyurethane/graphene foams in region of Ku-band [61]. PUG = polyurethane/graphene foam. Reproduced with permission from Elsevier.

Table 1. Electrical conductivity and EMI shielding effectiveness of polyurethane nanocomposite foam.

Nanocomposite Foam Matrix	Nanofiller	Conductivity	EMI Shielding Effectiveness	Ref.
Polyurethane	Reduced graphene oxide 3.17 vol.%	$2.53 \times 10^{-1} \text{ Sm}^{-1}$	22 dB	[57]
Polyurethane	Graphene oxide 20 wt.%	3 Scm^{-1}	17–24 dB	[61]
Polyurethane	Carbon nanotube	0.23 Scm^{-1}	-	[80]
Polyurethane	Carbon nanotube	Percolation threshold 1.2 wt.%; $2.03 \times 10^{-6} \text{ Sm}^{-1}$	-	[77]
Waterborne polyurethane	Carbon nanotube	362 Sm^{-1}	25 dB	[116]
Polyurethane	Reduced graphene oxide	4 Sm^{-1}	253 dB	[117]

4.3. Biomedical Field Applications

Polyurethanes have been considered an important polymer for biomedical applications [118]. Mainly properties of polyurethanes (biocompatibility, biodegradability, controllable chemical, physical properties) have been found to be effective for biomedical purposes [119]. Progress in the field of polyurethanes led to several innovative biomedical

areas ranging from drug delivery to tissue engineering [120]. Consequently, polyurethanes have been frequently used to form drug delivery carriers, stents, catheters, adhesives, coatings, bioimplants, and other tissue engineering scaffolds [121–123]. Accordingly, polyurethane foam materials have been developed and applied for numerous *in vivo* and *in vitro* uses [124,125]. Owing to *in vivo* or *in vitro* stability and bio sustainability of polyurethane foams, these materials have been preferred for long-life biomedical devices [126]. Guelcher and colleagues [127] fabricated polyurethane foams of lysine methyl ester diisocyanate and poly(ϵ -caprolactone-*co*-glycolide) triol reactants by tertiary amine catalyst. Polyurethane foam revealed fine *in vitro* biocompatibility of injectable scaffolds [128]. Schreder and co-workers [129] developed polyurethane-derived nanocomposite foams filled with hydroxyapatite nanoparticles. Nanocomposite foams had good biocompatibility for interaction with bone tissue cells. Hence, these polymer nanocomposite foams have good bone tissue engineering solicitations [130]. Zawadza et al. [131] formed carbon nanotube-coated polyurethane via the electrophoretic deposition method used for tissue engineering. In this study, the effect of nanotube coating on the bioactivity of polyurethane-based scaffolds has been assessed for the formation of calcium phosphate of hydroxyapatite on foam surfaces. The presence of carbon nanotubes acted as nucleation centers to facilitate the formation of hydroxyapatite in tissue engineering compared with non-coated foam samples. Hence, nanocarbon-coated polyurethane foams have been used as potential contenders to form bioactive scaffolds in bone tissue engineering owing to suitable porosity, bioactivity, and nanostructured topography. However, nanocarbon-based polyurethane nanocomposite foams have major issues in controlling the *in vivo* and *in vitro* toxicity levels [132]. Future research attempts with controlled toxicity levels may lead to further progress in this field. Moreover, polyurethane foams and nanocomposite foams have been found to be useful for injectable delivery systems [133]. In this context, polyurethane/graphene nanocomposite foam and polyurethane/carbon nanotube nanocomposite foam scaffolds have been designed and studied. Shin et al. [134] designed three-dimensional scaffolds based on polyurethane foams filled with graphene and graphene oxide nanosheets. Three-dimensional scaffolds were tested for facilitating the cell growth of skeletal tissues. Moreover, polyurethane nanocomposite foams were used as biomimetic scaffolds for skeletal tissue regeneration. The porous consistent foams have a pore size of around 300 μm . Nanocomposite foams offered a fine microenvironment for skeletal cell growth. The myogenic differentiation of skeletal cells was also observed for nanocomposite foams. According to the studies, polyurethane/graphene and polyurethane/graphene nanocomposite foams have a good myogenic stimulation influence on myoblasts. Hence, these nanocomposite foams have been found to be effective in designing three-dimensional biomimetic scaffolds for drug delivery carriers and different types of tissue engineering purposes. Moreover, careful future studies must be performed to analyze the harmful effects and long-term influence of nanocarbon-filled foams for biomedical applications.

5. Prospects

Polymeric foams have gained immense attention for their important methodological applications [135]. The addition of nanofillers caused significant enhancement in the essential characteristics of the polymeric foams [136]. Consequently, the microstructure, morphology, fabrication efficiency, as well as thermal, electrical, mechanical, and other technical features of filled polyurethane foams have been observed. In particular, the remarkable performances of carbon nanofillers (graphene, graphene oxide, carbon nanotube)-filled polymeric foams were investigated in the literature [137]. Polyurethanes have been considered important matrices for nanocomposite foam fabrication. Carbon nanofillers (graphene and carbon nanotube) filled polyurethane foams have been applied for shape memory spongy nanomaterials, EMI shielding foams, and biomedical relevance. However, there are several hidden future application areas of these high-performance polyurethane nanocomposite foam materials. For example, like other polymeric foams [137], polyurethane/graphene

and polyurethane/carbon nanotube foam materials can be employed in the space sector, especially for structural applications. High strength, non-flammability, and thermal conduction properties of polyurethane nanocomposite foams have been found to be effective in forming lightweight sandwich panels for space structures. Furthermore, the energy absorption features of these polyurethane nanocomposite foam-based sandwich panels may be explored for important utilizations. Similar to other polymeric foams [138], the non-flammability and mechanical strength properties of polyurethane nanocomposite foams were useful for high-tech automotive applications. Polymer foams have important applications in the construction industry [139]. Here again, polyurethane-derived nanocomposite foams can be used to support or develop buildings and structures. In particular, these foams may offer high strength and energetic radiation protection to building structures. Another important use of polyurethane nanocomposite foams has been observed for developing eco-friendly and sustainable materials [140].

6. Conclusions

Briefly, polyurethane has been researched as a multipurpose polymer to develop foam materials. Consequently, various thermoplastics or thermosetting polyurethane foams have been reported in the literature. Several chemical or physical foaming methods employing foaming agents, freeze drying, supercritical CO₂ foaming, compression molding, etc., have been adopted. Nanocarbon nanoparticles have been included for design, microstructural control, and overall enhancement in the physical performance of polyurethane foams. Unique pore structures, open or closed cell structures, electronic, mechanical, thermal, and other properties have been attained. Graphene and carbon nanotubes have played important roles in polyurethane foam reinforcement. Polyurethane and polyurethane nanocomposite foams were found to have good processing capabilities, chemical constancy, flexibility, compressibility, reversibility, heat stability, non-flammability, mechanical strength, electron conduction, thermal conductivity, and several other important physical characteristics. The inclusion of carbon nanoparticles in polyurethane foams has positively altered morphology, physical properties, and technical performance depending on nanofiller contents and the dispersion in the matrix. Noteworthy applications of polyurethane nanocomposite foams have been observed for stimuli responsiveness, EMI shielding, and biomedical uses. However, these application areas need to be further explored for future progress in the field of polyurethane/nanocarbon nanocomposite foams. Exploring current challenges associated with these foams may open future research pathways for significant technical applications.

Author Contributions: Conceptualization, A.K.; data curation, A.K.; writing of original draft preparation, A.K.; review and editing, A.K., I.A., T.Z., O.A., K.H.I. and M.H.E. All authors have read and agreed to the published version of the manuscript.

Funding: This work was supported and funded by the Deanship of Scientific Research at Imam Mohammad Ibn Saud Islamic University (IMSIU) (grant number IMSIU-RP23084).

Acknowledgments: The authors extend their appreciation to the Deanship of Scientific Research at Imam Mohammad Ibn Saud Islamic University (IMSIU) for supporting and supervising this project.

Conflicts of Interest: The authors declare no conflict of interest.

References

1. Xu, H.; Liu, D.; Liang, L.; Tian, Z.; Shen, P. Nitrogen-doped graphene sheets as efficient nanofillers at ultra-low content for reinforcing mechanical and wear-resistant properties of acrylic polyurethane coatings. *Crystals* **2022**, *12*, 1820. [[CrossRef](#)]
2. Fanali, S.; Tumedei, M.; Pignatelli, P.; Petrini, M.; Piattelli, A.; Iezzi, G. The effect of threads geometry on insertion torque (IT) and periosteal implant primary stability: A high-density polyurethane simulation for the anterior mandible. *Crystals* **2021**, *11*, 308. [[CrossRef](#)]
3. Zhang, C.; Kessler, M.R. Bio-based polyurethane foam made from compatible blends of vegetable-oil-based polyol and petroleum-based polyol. *ACS Sustain. Chem. Eng.* **2015**, *3*, 743–749. [[CrossRef](#)]

4. Engels, H.W.; Pirkel, H.G.; Albers, R.; Albach, R.W.; Krause, J.; Hoffmann, A.; Casselmann, H.; Dormish, J. Polyurethanes: Versatile materials and sustainable problem solvers for today's challenges. *Angew. Chem. Int. Ed.* **2013**, *52*, 9422–9441. [[CrossRef](#)]
5. Li, Z.; Zhang, R.; Moon, K.S.; Liu, Y.; Hansen, K.; Le, T.; Wong, C. Highly Conductive, Flexible, Polyurethane-Based Adhesives for Flexible and Printed Electronics. *Adv. Funct. Mater.* **2013**, *23*, 1459–1465. [[CrossRef](#)]
6. Shikha; Meena, M.; Jacob, J. Pentaerythritol derived phosphorous based bicyclic compounds as promising flame retardants for thermoplastic polyurethane films. *J. Appl. Polym. Sci.* **2020**, *138*, 50375. [[CrossRef](#)]
7. Du, Y.; Wang, M.; Ye, X.; Liu, B.; Han, L.; Jafri, S.H.M.; Liu, W.; Zheng, X.; Ning, Y.; Li, H. Advances in the Field of Graphene-Based Composites for Energy-Storage Applications. *Crystals* **2023**, *13*, 912. [[CrossRef](#)]
8. Sharif, M.; Heidari, A.; Aghaeinejad Meybodi, A. Polythiophene/Zinc Oxide/Graphene Oxide Ternary Photocatalyst: Synthesis, characterization and application. *Polym.-Plast. Technol. Mater.* **2021**, *60*, 1450–1460. [[CrossRef](#)]
9. Zhang, R.; Palumbo, A.; Kim, J.C.; Ding, J.; Yang, E.H. Flexible Graphene-, Graphene-Oxide-, and Carbon-Nanotube-Based Supercapacitors and Batteries. *Ann. Phys.* **2019**, *531*, 1800507. [[CrossRef](#)]
10. Ding, H.; Zhang, X. Sodium Intercalation in Nitrogen-Doped Graphene-Based Anode: A First-Principles Study. *Crystals* **2023**, *13*, 1011. [[CrossRef](#)]
11. Jibin, K.P.; Augustine, S.; Velayudhan, P.; George, J.S.; Krishnagesham Sidharthan, S.; Poullose, S.V.; Thomas, S. Unleashing the Power of Graphene-Based Nanomaterials for Chromium (VI) Ion Elimination from Water. *Crystals* **2023**, *13*, 1047. [[CrossRef](#)]
12. Zhang, X.; Xiang, D.; Zhu, W.; Zheng, Y.; Harkin-Jones, E.; Wang, P.; Zhao, C.; Li, H.; Wang, B.; Li, Y. Flexible and high-performance piezoresistive strain sensors based on carbon nanoparticles@ polyurethane sponges. *Compos. Sci. Technol.* **2020**, *200*, 108437. [[CrossRef](#)]
13. Zhang, H.; Zhang, G.; Li, J.; Fan, X.; Jing, Z.; Li, J.; Shi, X. Lightweight, multifunctional microcellular PMMA/Fe₃O₄@MWCNTs nanocomposite foams with efficient electromagnetic interference shielding. *Compos. Part A Appl. Sci. Manuf.* **2017**, *100*, 128–138. [[CrossRef](#)]
14. Gama, N.V.; Ferreira, A.; Barros-Timmons, A. Polyurethane foams: Past, present, and future. *Materials* **2018**, *11*, 1841. [[CrossRef](#)]
15. Yadav, A.; de Souza, F.M.; Dawsey, T.; Gupta, R.K. Recent advancements in flame-retardant polyurethane foams: A review. *Ind. Eng. Chem. Res.* **2022**, *61*, 15046–15065. [[CrossRef](#)]
16. Haridevan, H.; Evans, D.A.; Ragauskas, A.J.; Martin, D.J.; Annamalai, P.K. Valorisation of technical lignin in rigid polyurethane foam: A critical evaluation on trends, guidelines and future perspectives. *Green Chem.* **2021**, *23*, 8725–8753. [[CrossRef](#)]
17. Mohamad, M.; Abd Razak, J.; Mohamad, N.; Ahmad, S.H.; Junid, R.; Puspitasari, P. A short review on polyurethane-based nanocomposites for various applications. In Proceedings of the IOP Conference Series: Materials Science and Engineering, International Conference on Sustainable Materials (ICoSM 2020), Pahang, Malaysia, 30 March 2020; IOP Publishing: Bristol, UK, 2020; p. 012029.
18. Sang, G.; Xu, P.; Yan, T.; Murugadoss, V.; Naik, N.; Ding, Y.; Guo, Z. Interface engineered microcellular magnetic conductive polyurethane nanocomposite foams for electromagnetic interference shielding. *Nano-Micro Lett.* **2021**, *13*, 153. [[CrossRef](#)]
19. Ahmadijokani, F.; Molavi, H.; Ahmadipouya, S.; Rezakazemi, M.; Ghaffarkhah, A.; Kamkar, M.; Shojaei, A.; Arjmand, M. Polyurethane-based membranes for CO₂ separation: A comprehensive review. *Prog. Energy Combust. Sci.* **2023**, *97*, 101095. [[CrossRef](#)]
20. Chen, Q.; Wang, C.; Li, Y.; Feng, L.; Huang, S. Performance development of polyurethane elastomer composites in different construction and curing environments. *Constr. Build. Mater.* **2023**, *365*, 130047. [[CrossRef](#)]
21. Asensio, M.; Ferrer, J.-F.; Nohales, A.; Culebras, M.; Gómez, C.M. The Role of Diisocyanate Structure to Modify Properties of Segmented Polyurethanes. *Materials* **2023**, *16*, 1633. [[CrossRef](#)]
22. Mukhametshin, T.I.; Vinogradov, D.B.; Bulatov, P.V.; Nikitin, V.G.; Petrov, V.A. Synthesis of segmented polyurethanes based on furazan units. *Mendeleev Commun.* **2023**, *33*, 408–410. [[CrossRef](#)]
23. Chen, J.; Li, F.; Luo, Y.; Shi, Y.; Ma, X.; Zhang, M.; Boukhvalov, D.; Luo, Z. A self-healing elastomer based on an intrinsic non-covalent cross-linking mechanism. *J. Mater. Chem. A* **2019**, *7*, 15207–15214. [[CrossRef](#)]
24. Kaikade, D.S.; Sabnis, A.S. Polyurethane foams from vegetable oil-based polyols: A review. *Polym. Bull.* **2023**, *80*, 2239–2261. [[CrossRef](#)] [[PubMed](#)]
25. Luo, G.; Xie, J.; Liu, J.; Zhang, Q.; Luo, Y.; Li, M.; Zhou, W.; Chen, K.; Li, Z.; Yang, P. Highly conductive, stretchable, durable, breathable electrodes based on electrospun polyurethane mats superficially decorated with carbon nanotubes for multifunctional wearable electronics. *Chem. Eng. J.* **2023**, *451*, 138549. [[CrossRef](#)]
26. Gao, H.; Sun, Y.; Jian, J.; Dong, Y.; Liu, H. Study on mechanical properties and application in communication pole line engineering of glass fiber reinforced polyurethane composites (GFRP). *Case Stud. Constr. Mater.* **2023**, *18*, e01942. [[CrossRef](#)]
27. Choe, J.A.; Uthamaraj, S.; Dragomir-Daescu, D.; Sandhu, G.S.; Tefft, B.J. Magnetic and biocompatible polyurethane nanofiber biomaterial for tissue engineering. *Tissue Eng. Part A* **2023**. [[CrossRef](#)]
28. Recupido, F.; Lama, G.C.; Ammendola, M.; Bossa, F.D.L.; Minigher, A.; Campaner, P.; Morena, A.G.; Tzanov, T.; Ornelas, M.; Barros, A. Rigid composite bio-based polyurethane foams: From synthesis to LCA analysis. *Polymer* **2023**, *267*, 125674. [[CrossRef](#)]
29. Septevani, A.A.; Evans, D.A.; Chaleat, C.; Martin, D.J.; Annamalai, P.K. A systematic study substituting polyether polyol with palm kernel oil based polyester polyol in rigid polyurethane foam. *Ind. Crops Prod.* **2015**, *66*, 16–26. [[CrossRef](#)]
30. Marcovich, N.; Kurańska, M.; Prociak, A.; Malewska, E.; Kulpa, K. Open cell semi-rigid polyurethane foams synthesized using palm oil-based bio-polyol. *Ind. Crops Prod.* **2017**, *102*, 88–96. [[CrossRef](#)]

31. Kurańska, M.; Polaczek, K.; Auguścik-Królikowska, M.; Prociak, A.; Ryszkowska, J. Open-cell rigid polyurethane bio-foams based on modified used cooking oil. *Polymer* **2020**, *190*, 122164. [[CrossRef](#)]
32. Saint-Michel, F.; Chazeau, L.; Cavallé, J.-Y.; Chabert, E. Mechanical properties of high density polyurethane foams: I. Effect of the density. *Compos. Sci. Technol.* **2006**, *66*, 2700–2708. [[CrossRef](#)]
33. Langanke, J.; Wolf, A.; Hofmann, J.; Böhm, K.; Subhani, M.; Müller, T.; Leitner, W.; Gürtler, C. Carbon dioxide (CO₂) as sustainable feedstock for polyurethane production. *Green Chem.* **2014**, *16*, 1865–1870. [[CrossRef](#)]
34. Annaz, B.; Hing, K.; Kayser, M.; Buckland, T.; Silvio, L.D. Porosity variation in hydroxyapatite and osteoblast morphology: A scanning electron microscopy study. *J. Microsc.* **2004**, *215*, 100–110. [[CrossRef](#)] [[PubMed](#)]
35. Ling, Z.; Liu, J.; Wang, Q.; Lin, W.; Fang, X.; Zhang, Z. MgCl₂·6H₂O-Mg(NO₃)₂·6H₂O eutectic/SiO₂ composite phase change material with improved thermal reliability and enhanced thermal conductivity. *Sol. Energy Mater. Sol. Cells* **2017**, *172*, 195–201. [[CrossRef](#)]
36. Fu, W.; Zou, T.; Liang, X.; Wang, S.; Gao, X.; Zhang, Z.; Fang, Y. Thermal properties and thermal conductivity enhancement of composite phase change material using sodium acetate trihydrate-urea/expanded graphite for radiant floor heating system. *Appl. Therm. Eng.* **2018**, *138*, 618–626. [[CrossRef](#)]
37. Tan, S.; Abraham, T.; Ference, D.; Macosko, C.W. Rigid polyurethane foams from a soybean oil-based polyol. *Polymer* **2011**, *52*, 2840–2846. [[CrossRef](#)]
38. Zhang, Y.; Choi, J.R.; Park, S.-J. Interlayer polymerization in amine-terminated macromolecular chain-grafted expanded graphite for fabricating highly thermal conductive and physically strong thermoset composites for thermal management applications. *Compos. Part A Appl. Sci. Manuf.* **2018**, *109*, 498–506. [[CrossRef](#)]
39. Liu, L.; Wang, Z. High performance nano-zinc amino-tris-(methylenephosphonate) in rigid polyurethane foam with improved mechanical strength, thermal stability and flame retardancy. *Polym. Degrad. Stab.* **2018**, *154*, 62–72. [[CrossRef](#)]
40. Patil, A.; Patel, A.; Purohit, R. An overview of polymeric materials for automotive applications. *Mater. Today Proc.* **2017**, *4*, 3807–3815. [[CrossRef](#)]
41. Kausar, A. Role of thermosetting polymer in structural composite. *Am. J. Polym. Sci. Eng.* **2017**, *5*, 1–12.
42. Choong, P.S.; Hui, Y.L.E.; Lim, C.C. CO₂-Blown Nonisocyanate Polyurethane Foams. *ACS Macro Lett.* **2023**, *12*, 1094–1099. [[CrossRef](#)] [[PubMed](#)]
43. Soundhar, A.; Rajesh, M.; Jayakrishna, K.; Sultan, M.; Shah, A. Investigation on mechanical properties of polyurethane hybrid nanocomposite foams reinforced with roselle fibers and silica nanoparticles. *Nanocomposites* **2019**, *5*, 1–12. [[CrossRef](#)]
44. Bonab, S.A.; Moghaddas, J.; Rezaei, M. In-situ synthesis of silica aerogel/polyurethane inorganic-organic hybrid nanocomposite foams: Characterization, cell microstructure and mechanical properties. *Polymer* **2019**, *172*, 27–40. [[CrossRef](#)]
45. Bi, J.; Du, Z.; Sun, J.; Liu, Y.; Wang, K.; Du, H.; Ai, W.; Huang, W. On the Road to the Frontiers of Lithium-Ion Batteries: A Review and Outlook of Graphene Anodes. *Adv. Mater.* **2023**, *35*, 2210734. [[CrossRef](#)]
46. Garcia de Abajo, F.J. Graphene plasmonics: Challenges and opportunities. *ACS Photonics* **2014**, *1*, 135–152. [[CrossRef](#)]
47. Dimiev, A.M.; Tour, J.M. Mechanism of graphene oxide formation. *ACS Nano* **2014**, *8*, 3060–3068. [[CrossRef](#)]
48. Gupta, V.; Sharma, N.; Singh, U.; Arif, M.; Singh, A. Higher oxidation level in graphene oxide. *Optik* **2017**, *143*, 115–124. [[CrossRef](#)]
49. Hidayah, N.; Liu, W.-W.; Lai, C.-W.; Noriman, N.; Khe, C.-S.; Hashim, U.; Lee, H.C. Comparison on graphite, graphene oxide and reduced graphene oxide: Synthesis and characterization. In Proceedings of the International Conference of Global Network for Innovative Technology and Awam International Conference in Civil Engineering (IGNITE-AICCE'17): Sustainable Technology and Practice for Infrastructure and Community Resilience, Penang, Malaysia, 8–9 August 2017; AIP Publishing LLC: Melville, NY, USA, 2007; p. 150002.
50. Zhang, Y.; Wu, J.; Jia, L.; Qu, Y.; Yang, Y.; Jia, B.; Moss, D.J. Graphene oxide for nonlinear integrated photonics. *Laser Photonics Rev.* **2023**, *17*, 2200512. [[CrossRef](#)]
51. Tiwari, S.; Chhaunker, S.; Maiti, P. Bio-based polyurethane-graphene composites for adhesive application. *SPE Polym.* **2023**, *4*, 41–48. [[CrossRef](#)]
52. Kuila, T.; Bose, S.; Khanra, P.; Kim, N.H.; Rhee, K.Y.; Lee, J.H. Characterization and properties of in situ emulsion polymerized poly (methyl methacrylate)/graphene nanocomposites. *Compos. Part A Appl. Sci. Manuf.* **2011**, *42*, 1856–1861. [[CrossRef](#)]
53. Zhang, H.; Zhang, G.; Tang, M.; Zhou, L.; Li, J.; Fan, X.; Shi, X.; Qin, J. Synergistic effect of carbon nanotube and graphene nanoplates on the mechanical, electrical and electromagnetic interference shielding properties of polymer composites and polymer composite foams. *Chem. Eng. J.* **2018**, *353*, 381–393. [[CrossRef](#)]
54. Yan, D.; Xu, L.; Chen, C.; Tang, J.; Ji, X.; Li, Z. Enhanced mechanical and thermal properties of rigid polyurethane foam composites containing graphene nanosheets and carbon nanotubes. *Polym. Int.* **2012**, *61*, 1107–1114. [[CrossRef](#)]
55. Ramasamy, R.P.; Somanathan, S.; Rafailovich, M.H.; Aswal, V.K. Broadband dielectric spectroscopy and small-angle neutron scattering investigations of polyurethane-graphene foams. *J. Mater. Sci. Mater. Electron.* **2020**, *31*, 15843–15851. [[CrossRef](#)]
56. Mundinamani, S. The choice of noble electrolyte for symmetric polyurethane-graphene composite supercapacitors. *Int. J. Hydrogen Energy* **2019**, *44*, 11240–11246. [[CrossRef](#)]
57. Jiang, Q.; Liao, X.; Li, J.; Chen, J.; Wang, G.; Yi, J.; Yang, Q.; Li, G. Flexible thermoplastic polyurethane/reduced graphene oxide composite foams for electromagnetic interference shielding with high absorption characteristic. *Compos. Part A Appl. Sci. Manuf.* **2019**, *123*, 310–319. [[CrossRef](#)]

58. Zaaba, N.; Foo, K.; Hashim, U.; Tan, S.; Liu, W.-W.; Voon, C. Synthesis of graphene oxide using modified hummers method: Solvent influence. *Procedia Eng.* **2017**, *184*, 469–477. [[CrossRef](#)]
59. Tas, M.; Altin, Y.; Bedeloglu, A.C. Reduction of graphene oxide thin films using a stepwise thermal annealing assisted by L-ascorbic acid. *Diam. Relat. Mater.* **2019**, *92*, 242–247. [[CrossRef](#)]
60. Li, J.; Liao, X.; Han, W.; Xiao, W.; Ye, J.; Yang, Q.; Li, G.; Ran, Q. Microcellular nanocomposites based on millable polyurethane and nano-silica by two-step curing and solid-state supercritical CO₂ foaming: Preparation, high-pressure viscoelasticity and mechanical properties. *J. Supercrit. Fluids* **2017**, *130*, 198–209. [[CrossRef](#)]
61. Li, Y.; Shen, B.; Yi, D.; Zhang, L.; Zhai, W.; Wei, X.; Zheng, W. The influence of gradient and sandwich configurations on the electromagnetic interference shielding performance of multilayered thermoplastic polyurethane/graphene composite foams. *Compos. Sci. Technol.* **2017**, *138*, 209–216. [[CrossRef](#)]
62. Feng, C.; Yi, Z.; Jin, X.; Seraji, S.M.; Dong, Y.; Kong, L.; Salim, N. Solvent crystallization-induced porous polyurethane/graphene composite foams for pressure sensing. *Compos. Part B Eng.* **2020**, *194*, 108065. [[CrossRef](#)]
63. Chen, Y.; Li, Y.; Xu, D.; Zhai, W. Fabrication of stretchable, flexible conductive thermoplastic polyurethane/graphene composites via foaming. *RSC Adv.* **2015**, *5*, 82034–82041. [[CrossRef](#)]
64. Hodlur, R.; Rabinal, M. Self assembled graphene layers on polyurethane foam as a highly pressure sensitive conducting composite. *Compos. Sci. Technol.* **2014**, *90*, 160–165. [[CrossRef](#)]
65. Ola, O.; Chen, Y.; Zhu, Y. Three-dimensional carbon foam nanocomposites for thermal energy storage. *Sol. Energy Mater. Sol. Cells* **2019**, *191*, 297–305. [[CrossRef](#)]
66. Kim, J.M.; Kim, D.H.; Kim, J.; Lee, J.W.; Kim, W.N. Effect of graphene on the sound damping properties of flexible polyurethane foams. *Macromol. Res.* **2017**, *25*, 190–196. [[CrossRef](#)]
67. Qin, L.-C.; Zhao, X.; Hirahara, K.; Miyamoto, Y.; Ando, Y.; Iijima, S. The smallest carbon nanotube. *Nature* **2000**, *408*, 50. [[CrossRef](#)]
68. Abubakre, O.K.; Medupin, R.O.; Akintunde, I.B.; Jimoh, O.T.; Abdulkareem, A.S.; Muriana, R.A.; James, J.A.; Ukoba, K.O.; Jen, T.-C.; Yoro, K.O. Carbon nanotube-reinforced polymer nanocomposites for sustainable biomedical applications: A review. *J. Sci. Adv. Mater. Devices* **2023**, *8*, 100557. [[CrossRef](#)]
69. Wei, M.; Robin, M.; Portilla, L.; Ren, Y.; Shao, S.; Bai, L.; Cao, Y.; Pecunia, V.; Cui, Z.; Zhao, J. Air-stable N-type printed carbon nanotube thin film transistors for CMOS logic circuits. *Carbon* **2020**, *163*, 145–153. [[CrossRef](#)]
70. Wang, R.; Sun, L.; Zhu, X.; Ge, W.; Li, H.; Li, Z.; Zhang, H.; Huang, Y.; Li, Z.; Zhang, Y.F. Carbon nanotube-based strain sensors: Structures, fabrication, and applications. *Adv. Mater. Technol.* **2023**, *8*, 2200855. [[CrossRef](#)]
71. Koziol, K.; Vilatela, J.; Moisala, A.; Motta, M.; Cunniff, P.; Sennett, M.; Windle, A. High-performance carbon nanotube fiber. *Science* **2007**, *318*, 1892–1895. [[CrossRef](#)]
72. Dong, F.; Yang, X.; Guo, L.; Qian, Y.; Sun, P.; Huang, Z.; Xu, X.; Liu, H. A tough, healable, and recyclable conductive polyurethane/carbon nanotube composite. *J. Colloid Interface Sci.* **2023**, *631*, 239–248. [[CrossRef](#)]
73. Zeng, C.; Hossieny, N.; Zhang, C.; Wang, B. Synthesis and processing of PMMA carbon nanotube nanocomposite foams. *Polymer* **2010**, *51*, 655–664. [[CrossRef](#)]
74. Wang, X.; Qu, M.; Wu, K.; Schubert, D.W.; Liu, X. High sensitive electrospun thermoplastic polyurethane/carbon nanotubes strain sensor fitting by a novel optimization empirical model. *Adv. Compos. Hybrid Mater.* **2023**, *6*, 63. [[CrossRef](#)]
75. Wang, G.; Wang, M.; Zheng, M.; Ebo, B.; Xu, C.; Liu, Z.; He, L. Thermoplastic Polyurethane/Carbon Nanotube Composites for Stretchable Flexible Pressure Sensors. *ACS Appl. Nano Mater.* **2023**, *6*, 9865–9873. [[CrossRef](#)]
76. Huang, W.; Dai, K.; Zhai, Y.; Liu, H.; Zhan, P.; Gao, J.; Zheng, G.; Liu, C.; Shen, C. Flexible and lightweight pressure sensor based on carbon nanotube/thermoplastic polyurethane-aligned conductive foam with superior compressibility and stability. *ACS Appl. Mater. Interfaces* **2017**, *9*, 42266–42277. [[CrossRef](#)]
77. Yan, D.X.; Dai, K.; Xiang, Z.D.; Li, Z.M.; Ji, X.; Zhang, W.Q. Electrical conductivity and major mechanical and thermal properties of carbon nanotube-filled polyurethane foams. *J. Appl. Polym. Sci.* **2011**, *120*, 3014–3019. [[CrossRef](#)]
78. Fan, Q.; Qin, Z.; Gao, S.; Wu, Y.; Pionteck, J.; Mäder, E.; Zhu, M. The use of a carbon nanotube layer on a polyurethane multifilament substrate for monitoring strains as large as 400%. *Carbon* **2012**, *50*, 4085–4092. [[CrossRef](#)]
79. Ramôa, S.D.; Barra, G.M.; Oliveira, R.V.; de Oliveira, M.G.; Cossa, M.; Soares, B.G. Electrical, rheological and electromagnetic interference shielding properties of thermoplastic polyurethane/carbon nanotube composites. *Polym. Int.* **2013**, *62*, 1477–1484. [[CrossRef](#)]
80. You, K.M.; Park, S.S.; Lee, C.S.; Kim, J.M.; Park, G.P.; Kim, W.N. Preparation and characterization of conductive carbon nanotube-polyurethane foam composites. *J. Mater. Sci.* **2011**, *46*, 6850–6855. [[CrossRef](#)]
81. Al-Saleh, M.H. Electrically conductive carbon nanotube/polypropylene nanocomposite with improved mechanical properties. *Mater. Des.* **2015**, *85*, 76–81. [[CrossRef](#)]
82. Ahn, C.; Kim, S.-M.; Jung, J.-W.; Park, J.; Kim, T.; Lee, S.E.; Jang, D.; Hong, J.-W.; Han, S.M.; Jeon, S. Multifunctional polymer nanocomposites reinforced by 3D continuous ceramic nanofillers. *ACS Nano* **2018**, *12*, 9126–9133. [[CrossRef](#)]
83. Madaleno, L.; Pyrz, R.; Crosky, A.; Jensen, L.R.; Rauhe, J.C.M.; Dolomanova, V.; de Barros, A.M.M.V.; Pinto, J.J.C.; Norman, J. Processing and characterization of polyurethane nanocomposite foam reinforced with montmorillonite-carbon nanotube hybrids. *Compos. Part A Appl. Sci. Manuf.* **2013**, *44*, 1–7. [[CrossRef](#)]
84. Zhai, T.; Li, D.; Fei, G.; Xia, H. Piezoresistive and compression resistance relaxation behavior of water blown carbon nanotube/polyurethane composite foam. *Compos. Part A Appl. Sci. Manuf.* **2015**, *72*, 108–114. [[CrossRef](#)]

85. Feng, D.; Liu, P.; Wang, Q. Selective Microwave Sintering to Prepare Multifunctional Poly (ether imide) Bead Foams Based on Segregated Carbon Nanotube Conductive Network. *Ind. Eng. Chem. Res.* **2020**, *59*, 5838–5847. [[CrossRef](#)]
86. De Luca Bossa, F.; Santillo, C.; Verdolotti, L.; Campaner, P.; Minigher, A.; Boggioni, L.; Losio, S.; Coccia, F.; Iannace, S.; Lama, G.C. Greener nanocomposite polyurethane foam based on sustainable polyol and natural fillers: Investigation of chemico-physical and mechanical properties. *Materials* **2020**, *13*, 211. [[CrossRef](#)]
87. Wang, T.; Yu, W.-C.; Sun, W.-J.; Jia, L.-C.; Gao, J.-F.; Tang, J.-H.; Su, H.-J.; Yan, D.-X.; Li, Z.-M. Healable polyurethane/carbon nanotube composite with segregated structure for efficient electromagnetic interference shielding. *Compos. Sci. Technol.* **2020**, *200*, 108446. [[CrossRef](#)]
88. Patle, V.K.; Kumar, R.; Sharma, A.; Dwivedi, N.; Muchhala, D.; Chaudhary, A.; Mehta, Y.; Mondal, D.; Srivastava, A. Three dimension phenolic resin derived carbon-CNTs hybrid foam for fire retardant and effective electromagnetic interference shielding. *Compos. Part C Open Access* **2020**, *2*, 100020. [[CrossRef](#)]
89. Espadas-Escalante, J.; Avilés, F.; Gonzalez-Chi, P.; Oliva, A. Thermal conductivity and flammability of multiwall carbon nanotube/polyurethane foam composites. *J. Cell. Plast.* **2017**, *53*, 215–230. [[CrossRef](#)]
90. Holder, K.M.; Cain, A.A.; Plummer, M.G.; Stevens, B.E.; Odenborg, P.K.; Morgan, A.B.; Grunlan, J.C. Carbon nanotube multilayer nano-coatings prevent flame spread on flexible polyurethane foam. *Macromol. Mater. Eng.* **2016**, *301*, 665–673. [[CrossRef](#)]
91. Akbari-Azar, S.; Baghani, M.; Zakerzadeh, M.-R.; Shahsavari, H.; Sohrabpour, S. Analytical investigation of composite sandwich beams filled with shape memory polymer corrugated core. *Meccanica* **2019**, *54*, 1647–1661. [[CrossRef](#)]
92. Del Nero, D.; Joshi-Imre, A.; Voit, W. Measuring the Electric Properties of Thin Film Shape Memory Polymers in Simulated Physiological Conditions. In Proceedings of the 2019 IEEE 69th Electronic Components and Technology Conference (ECTC), Las Vegas, NV, USA, 28–31 May 2019; IEEE: Piscataway, NJ, USA, 2019; pp. 1848–1852.
93. Zheng, N.; Fang, Z.; Zou, W.; Zhao, Q.; Xie, T. Thermoset shape-memory polyurethane with intrinsic plasticity enabled by transcarbamoylation. *Angew. Chem.* **2016**, *128*, 11593–11597. [[CrossRef](#)]
94. Kim, N.E.; Park, S.; Kim, S.; Choi, J.H.; Kim, S.E.; Choe, S.H.; Kang, T.w.; Song, J.E.; Khang, G. Development of Gelatin-Based Shape-Memory Polymer Scaffolds with Fast Responsive Performance and Enhanced Mechanical Properties for Tissue Engineering Applications. *ACS Omega* **2023**, *8*, 6455–6462. [[CrossRef](#)] [[PubMed](#)]
95. Leng, J.; Lu, H.; Liu, Y.; Huang, W.M.; Du, S. Shape-memory polymers—A class of novel smart materials. *MRS Bull.* **2009**, *34*, 848–855. [[CrossRef](#)]
96. Pineda-Castillo, S.A.; Stiles, A.M.; Bohnstedt, B.N.; Lee, H.; Liu, Y.; Lee, C.-H. Shape Memory Polymer-Based Endovascular Devices: Design Criteria and Future Perspective. *Polymers* **2022**, *14*, 2526. [[CrossRef](#)] [[PubMed](#)]
97. Hager, M.D.; Bode, S.; Weber, C.; Schubert, U.S. Shape memory polymers: Past, present and future developments. *Prog. Polym. Sci.* **2015**, *49*, 3–33. [[CrossRef](#)]
98. Zhao, X.; Guo, B.; Wu, H.; Liang, Y.; Ma, P.X. Injectable antibacterial conductive nanocomposite cryogels with rapid shape recovery for noncompressible hemorrhage and wound healing. *Nat. Commun.* **2018**, *9*, 2784. [[CrossRef](#)]
99. Peterson, G.I.; Dobrynin, A.V.; Becker, M.L. Biodegradable shape memory polymers in medicine. *Adv. Healthc. Mater.* **2017**, *6*, 1700694. [[CrossRef](#)]
100. Rodriguez, J.N.; Zhu, C.; Duoss, E.B.; Wilson, T.S.; Spadaccini, C.M.; Lewicki, J.P. Shape-morphing composites with designed micro-architectures. *Sci. Rep.* **2016**, *6*, 27933. [[CrossRef](#)]
101. Singhal, P.; Rodriguez, J.N.; Small, W.; Eagleston, S.; Van de Water, J.; Maitland, D.J.; Wilson, T.S. Ultra low density and highly crosslinked biocompatible shape memory polyurethane foams. *J. Polym. Sci. Part B Polym. Phys.* **2012**, *50*, 724–737. [[CrossRef](#)]
102. Berg, G.J.; McBride, M.K.; Wang, C.; Bowman, C.N. New directions in the chemistry of shape memory polymers. *Polymer* **2014**, *55*, 5849–5872. [[CrossRef](#)]
103. Kausar, A.; Ur Rahman, A. Effect of graphene nanoplatelet addition on properties of thermo-responsive shape memory polyurethane-based nanocomposite. *Fuller. Nanotub. Carbon Nanostruct.* **2016**, *24*, 235–242. [[CrossRef](#)]
104. Kim, H.M.; Park, J.; Huang, Z.M.; Youn, J.R.; Song, Y.S. Carbon nanotubes embedded shape memory polyurethane foams. *Macromol. Res.* **2019**, *27*, 919–925. [[CrossRef](#)]
105. Kang, S.; Kwon, S.; Park, J.; Kim, B. Carbon nanotube reinforced shape memory polyurethane foam. *Polym. Bull.* **2013**, *70*, 885–893. [[CrossRef](#)]
106. Tobushi, H.; Shimada, D.; Hayashi, S.; Endo, M. Shape fixity and shape recovery of polyurethane shape-memory polymer foams. *Proc. Inst. Mech. Eng. Part L J. Mater. Des. Appl.* **2003**, *217*, 135–143. [[CrossRef](#)]
107. Kinkelaar, M.R.; Critchfield, F.E.; Lambach, J.L. One-Shot Cold Molded Flexible Polyurethane Foam from Low Primary Hydroxyl Polyols and Process for the Preparation Thereof. U.S. Patent 5,668,191, 16 September 1997.
108. Kausar, A. Shape memory polyurethane/graphene nanocomposites: Structures, properties, and applications. *J. Plast. Film. Sheeting* **2020**, *36*, 151–166. [[CrossRef](#)]
109. Zhou, J.; Li, H.; Liu, W.; Dugnani, R.; Tian, R.; Xue, W.; Chen, Y.; Guo, Y.; Duan, H.; Liu, H. A facile method to fabricate polyurethane based graphene foams/epoxy/carbon nanotubes composite for electro-active shape memory application. *Compos. Part A Appl. Sci. Manuf.* **2016**, *91*, 292–300. [[CrossRef](#)]
110. Serrano, M.C.; Ameer, G.A. Recent insights into the biomedical applications of shape-memory polymers. *Macromol. Biosci.* **2012**, *12*, 1156–1171. [[CrossRef](#)]

111. Guitart, J.; Carrera, D.; Beltran, V.; Torres, J.; Ayguadé, E. Dynamic CPU provisioning for self-managed secure web applications in SMP hosting platforms. *Comput. Netw.* **2008**, *52*, 1390–1409. [[CrossRef](#)]
112. Yu, K.; Yin, W.; Liu, Y.; Leng, J. Application of SMP composite in designing a morphing wing. In Proceedings of the ICEM 2008: International Conference on Experimental Mechanics 2008, Nanjing, China, 8–11 November 2008; SPIE: Bellingham, WA, USA, 2009; pp. 1367–1372.
113. Ghosh, S.; Ganguly, S.; Remanan, S.; Mondal, S.; Jana, S.; Maji, P.K.; Singha, N.; Das, N.C. Ultra-light weight, water durable and flexible highly electrical conductive polyurethane foam for superior electromagnetic interference shielding materials. *J. Mater. Sci. Mater. Electron.* **2018**, *29*, 10177–10189. [[CrossRef](#)]
114. Shen, B.; Li, Y.; Zhai, W.; Zheng, W. Compressible graphene-coated polymer foams with ultralow density for adjustable electromagnetic interference (EMI) shielding. *ACS Appl. Mater. Interfaces* **2016**, *8*, 8050–8057. [[CrossRef](#)]
115. Yang, J.; Liao, X.; Wang, G.; Chen, J.; Guo, F.; Tang, W.; Wang, W.; Yan, Z.; Li, G. Gradient structure design of lightweight and flexible silicone rubber nanocomposite foam for efficient electromagnetic interference shielding. *Chem. Eng. J.* **2020**, *390*, 124589. [[CrossRef](#)]
116. Li, H.; Yuan, D.; Li, P.; He, C. High conductive and mechanical robust carbon nanotubes/waterborne polyurethane composite films for efficient electromagnetic interference shielding. *Compos. Part A Appl. Sci. Manuf.* **2019**, *121*, 411–417. [[CrossRef](#)]
117. Gavgani, J.N.; Adelnia, H.; Zaarei, D.; Gudarzi, M.M. Lightweight flexible polyurethane/reduced ultralarge graphene oxide composite foams for electromagnetic interference shielding. *RSC Adv.* **2016**, *6*, 27517–27527. [[CrossRef](#)]
118. Wang, P.; Pyo, S.-H.; Zhu, W.; Hwang, H.; Chen, S. 3D Printing of Polyurethanes for Biomedical Applications. In *Emerging Technologies in Biophysical Sciences: A World Scientific Reference: Volume 1: Emerging Technologies for Biofabrication and Biomanufacturing*; World Scientific: Singapore, 2023; pp. 389–406.
119. Joseph, J.; Patel, R.; Wenham, A.; Smith, J. Biomedical applications of polyurethane materials and coatings. *Trans. IMF* **2018**, *96*, 121–129. [[CrossRef](#)]
120. Barrioni, B.R.; de Carvalho, S.M.; Oréface, R.L.; de Oliveira, A.A.R.; de Magalhães Pereira, M. Synthesis and characterization of biodegradable polyurethane films based on HDI with hydrolyzable crosslinked bonds and a homogeneous structure for biomedical applications. *Mater. Sci. Eng. C* **2015**, *52*, 22–30. [[CrossRef](#)]
121. Batool, J.A.; Rehman, K.; Qader, A.; Akash, M.S. Biomedical Applications of Carbohydrate-Based Polyurethane: From Biosynthesis to Degradation. *Curr. Pharm. Des.* **2022**, *28*, 1669–1687. [[CrossRef](#)] [[PubMed](#)]
122. Singh, J.; Singh, S.; Gill, R. Applications of biopolymer coatings in biomedical engineering. *J. Electrochem. Sci. Eng.* **2023**, *13*, 63–81. [[CrossRef](#)]
123. Ye, H.; Zhang, K.; Kai, D.; Li, Z.; Loh, X.J. Polyester elastomers for soft tissue engineering. *Chem. Soc. Rev.* **2018**, *47*, 4545–4580. [[CrossRef](#)]
124. Jetté, B.; Brailovski, V.; Simoneau, C.; Dumas, M.; Terriault, P. Development and in vitro validation of a simplified numerical model for the design of a biomimetic femoral stem. *J. Mech. Behav. Biomed. Mater.* **2018**, *77*, 539–550. [[CrossRef](#)]
125. Ribeiro, C.; Sencadas, V.; Correia, D.M.; Lanceros-Méndez, S. Piezoelectric polymers as biomaterials for tissue engineering applications. *Colloids Surf. B Biointerfaces* **2015**, *136*, 46–55. [[CrossRef](#)]
126. Caba, V.; Borgese, L.; Agnelli, S.; Depero, L.E. A green and simple process to develop conductive polyurethane foams for biomedical applications. *Int. J. Polym. Mater. Polym. Biomater.* **2019**, *68*, 126–133. [[CrossRef](#)]
127. Guelcher, S.A.; Patel, V.; Gallagher, K.M.; Connolly, S.; Didier, J.E.; Doctor, J.S.; Hollinger, J.O. Synthesis and in vitro biocompatibility of injectable polyurethane foam scaffolds. *Tissue Eng.* **2006**, *12*, 1247–1259. [[CrossRef](#)]
128. Pina, S.; Oliveira, J.M.; Reis, R.L. Natural-based nanocomposites for bone tissue engineering and regenerative medicine: A review. *Adv. Mater.* **2015**, *27*, 1143–1169. [[CrossRef](#)]
129. Schreuder, K.J.; Bayer, I.S.; Milner, D.J.; Loth, E.; Jasiuk, I. A polyurethane-based nanocomposite biocompatible bone adhesive. *J. Appl. Polym. Sci.* **2013**, *127*, 4974–4982. [[CrossRef](#)]
130. Hafeman, A.E.; Li, B.; Yoshii, T.; Zienkiewicz, K.; Davidson, J.M.; Guelcher, S.A. Injectable biodegradable polyurethane scaffolds with release of platelet-derived growth factor for tissue repair and regeneration. *Pharm. Res.* **2008**, *25*, 2387–2399. [[CrossRef](#)] [[PubMed](#)]
131. Zawadzak, E.; Bil, M.; Ryszkowska, J.; Nazhat, S.N.; Cho, J.; Bretcanu, O.; Roether, J.A.; Boccaccini, A.R. Polyurethane foams electrophoretically coated with carbon nanotubes for tissue engineering scaffolds. *Biomed. Mater.* **2008**, *4*, 015008. [[CrossRef](#)] [[PubMed](#)]
132. Chetyrkina, M.R.; Fedorov, F.S.; Nasibulin, A.G. In vitro toxicity of carbon nanotubes: A systematic review. *RSC Adv.* **2022**, *12*, 16235–16256. [[CrossRef](#)] [[PubMed](#)]
133. Cherng, J.Y.; Hou, T.Y.; Shih, M.F.; Talsma, H.; Hennink, W.E. Polyurethane-based drug delivery systems. *Int. J. Pharm.* **2013**, *450*, 145–162. [[CrossRef](#)]
134. Shin, Y.C.; Kang, S.H.; Lee, J.H.; Kim, B.; Hong, S.W.; Han, D.-W. Three-dimensional graphene oxide-coated polyurethane foams beneficial to myogenesis. *J. Biomater. Sci. Polym. Ed.* **2018**, *29*, 762–774. [[CrossRef](#)]
135. Rahimidehghan, F.; Altenhof, W. Compressive behavior and deformation mechanisms of rigid polymeric foams: A review. *Compos. Part B Eng.* **2023**, *253*, 110513. [[CrossRef](#)]
136. Harun-Ur-Rashid, M.; Imran, A.B.; Susan, M.A.B.H. Fire-Resistant Polymeric Foams and Their Applications. In *Polymeric Foams: Applications of Polymeric Foams (Volume 2)*; ACS Publications: Washington, DC, USA, 2023; pp. 97–121.

137. Banerjee, R.; Gebrekrestos, A.; Orasugh, J.T.; Ray, S.S. Nanocarbon-Containing Polymer Composite Foams: A Review of Systems for Applications in Electromagnetic Interference Shielding, Energy Storage, and Piezoresistive Sensors. *Ind. Eng. Chem. Res.* **2023**, *62*, 6807–6842. [[CrossRef](#)]
138. Adlie, T.A.; Ali, N.; Huzni, S.; Ikramullah, I.; Rizal, S. Impact of Zinc Oxide Addition on Oil Palm Empty Fruit Bunches Foamed Polymer Composites for Automotive Interior Parts. *Polymers* **2023**, *15*, 422. [[CrossRef](#)]
139. Kong, W.; Li, R.; Zhao, X.; Ye, L. Construction of a Highly Oriented Poly (lactic acid)-Based Block Polymer Foam and Its Self-Reinforcing Mechanism. *ACS Sustain. Chem. Eng.* **2023**, *11*, 1133–1145. [[CrossRef](#)]
140. Reddy, M.M.; Vivekanandhan, S.; Misra, M.; Bhatia, S.K.; Mohanty, A.K. Biobased plastics and bionanocomposites: Current status and future opportunities. *Prog. Polym. Sci.* **2013**, *38*, 1653–1689. [[CrossRef](#)]

Disclaimer/Publisher’s Note: The statements, opinions and data contained in all publications are solely those of the individual author(s) and contributor(s) and not of MDPI and/or the editor(s). MDPI and/or the editor(s) disclaim responsibility for any injury to people or property resulting from any ideas, methods, instructions or products referred to in the content.